

Multipartite Gaussian entanglement measure with applications to graph states and bosonic field theory

Matteo Gori* , Matthieu Sarkis and Alexandre Tkatchenko

Department of Physics and Materials Science, University of Luxembourg, L-1511 Luxembourg City, Luxembourg

E-mail: matteo.gori@uni.lu, matthieu.sarkis@uni.lu and alexandre.tkatchenko@uni.lu

Received 4 August 2025; revised 9 November 2025

Accepted for publication 19 November 2025

Published 5 December 2025



CrossMark

Abstract

Computationally feasible multipartite entanglement measures are essential for advancing our understanding of complex quantum systems. Entanglement distance (ED), introduced by Cocchiarella *et al* (2020 *Phys. Rev. A* **101** 042129), based on the Fubini–Study metric, offers several advantages over existing methods, including ease of computation, a profound geometrical interpretation, and applicability to multipartite entanglement. Although ED has been successfully applied to systems of qudits, an explicit formulation for continuous quantum variables, particularly for pure Gaussian states, remains unexplored. In this work, we address this limitation by deriving the analytical expression for the Gaussian entanglement measure (GEM), a multipartite entanglement monotone for multimode pure Gaussian states based on the purity of fragments of the whole system, through a generalization of ED to group-theoretic coherent states. We show the efficacy of GEM across various scenarios, including the analysis of a two-mode Gaussian state under beam-splitter and squeezing transformations, and exploring graph states involving three and four modes. Notably, comparing GEM values for states with different graph topologies reveals insights into the connectivity of the underlying graphs. Additionally, we illustrate how GEM provides insights into free bosonic field theory on $\mathbb{R}_t \times S^1$ beyond standard bipartite entanglement entropy, paving the way for quantum information-theoretic tools to probe the topological properties of quantum field theories.

* Author to whom any correspondence should be addressed.

Supplementary material for this article is available [online](#)

Keywords: quantum entanglement, quantum correlations, entanglement distance, generalized coherent states, graph states, bosonic field theory

Quantum entanglement stands as a cornerstone in the development of quantum-based technologies due to its significance in the pursuit of quantum supremacy [2, 3] and enhanced quantum control [4, 5]. Considerable strides have been made in comprehending quantum entanglement and its robustness within the mathematical framework of quantum information theory, encompassing both pure and mixed states [6, 7]. However, accurately quantifying entanglement continues to pose a significant unresolved challenge [8–12]. Historically, quantifying entanglement has centered on entropy-based measures. For instance, in pure and bipartite systems, the entropy of entanglement has been commonly acknowledged as a key measure of entanglement [13–15]. Faithful measures for mixed states of the same class of system include the entropy of formation [16], the entropy of distillation [13], and relative entropy of entanglement [8, 17, 18]. Yet, extending these measures to encompass broader classes of quantum states, especially in multipartite systems, requires exploring diverse methodologies [19–23]. Several measures, including the Schmidt measure [24] and generalized concurrence [25], have been proposed for multipartite systems, applicable to both pure and mixed states. The quest for a precisely defined entanglement measure capable of capturing multipartite entanglement across a wide range of systems beyond qubits, including both pure and mixed states, has prompted the investigation of novel approaches for deriving such measures. Recently, methods for estimating quantum entanglement and quantifying complexity in multipartite systems have emerged, leveraging insights from information geometry, particularly the quantum Fisher information [26–28].

More recently, a multipartite entanglement measure, called entanglement distance (ED) [1, 29–31] has been proposed in the form of an entanglement monotone derived from the Fubini–Study metric defined on the projective Hilbert space of the pure quantum states of a system of M qudit states. Extensions of the ED have been presented to include mixed states [29].

The ED presents numerous advantages with respect to other multipartite entanglement monotones. From a conceptual point of view, it naturally provides a differential geometrical framework to describe quantum entanglement [30, 31]. From a computational point of view, the ED for a given pure state is *a priori* much more efficient with respect to other multipartite entanglement measures, as it does not require the optimization over a set of separable states, but just the evaluation of a set of observables (i.e. products of the generators of the group of local operations (LOs)) on the considered state. Applications of the ED have been presented for graph states [31] and to the characterization of the entanglement protection of qubits in lossy cavities [32]. While, in principle, a similar construction could be done in the case of continuous variable quantum systems, no extensive studies have been done so far in this direction. Gaussian states hold a pivotal position among the manifold of states linked to continuous quantum variables. They are known by various names (such as squeezed coherent states, generalized Slater determinants, and ground states of quadratic Hamiltonians) and find utility across diverse research domains, including quantum information [33–36], in quantum field theory in curved spacetime [37, 38] and in thermofield dynamics [39, 40]. In particular, Gaussian states constitute a manifold of states in (projective) Hilbert space often used to approximate ground states for complicated Hamiltonians through variational methods [41–44]. Furthermore, numerous quantum information techniques can be analytically applied to Gaussian states, including computations of entanglement entropy [45, 46], logarithmic negativity [47–49], and circuit complexity [50, 51]). Finally, recent studies in mathematical

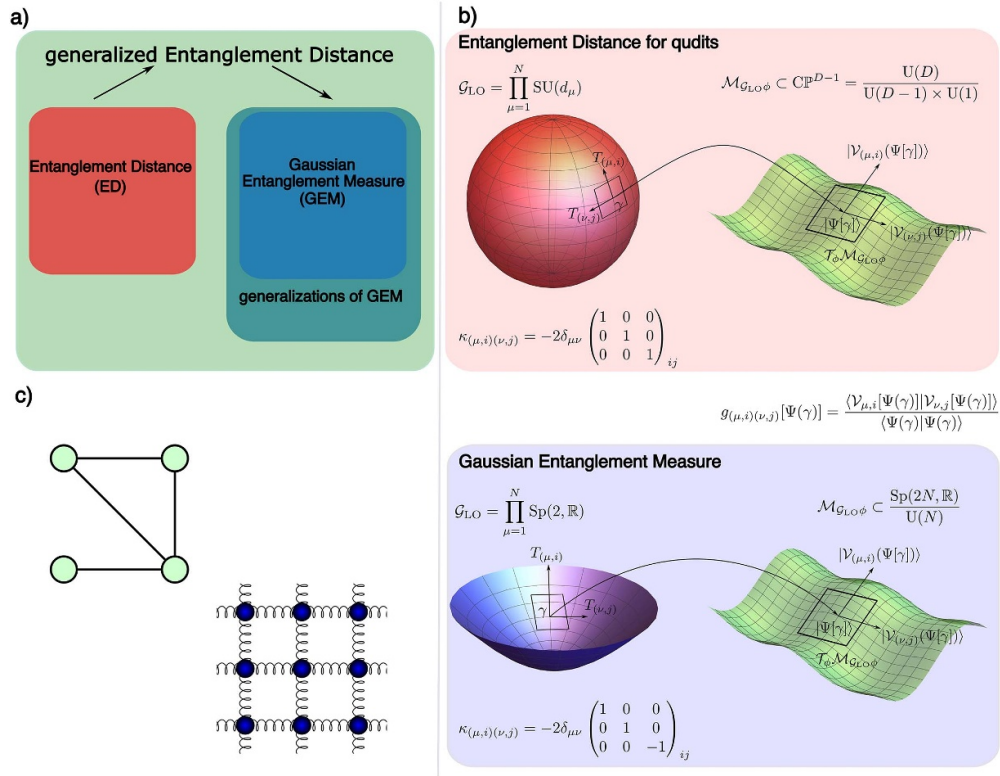


Figure 1. Gaussian entanglement measure: concepts and applications in panel (a), illustration of the path followed in the paper to derive the Gaussian entanglement measure from the entanglement distance (ED) introduced in [1]: reformulation and generalization of the ED in the framework of group-theoretic coherent states, and definition of the GEM. In panel (b), schematic illustration of the geometric construction involved in the paper. In the context of group-theoretic coherent states, we obtain the generalized ED of a given state $|\Psi\rangle$ by contracting the inverse of the Killing form $k_{(\mu,i)(\nu,j)}$ with the Fubini–Study metric $g_{(\mu,i)(\nu,j)}$ defined on the manifold $\mathcal{M}_{\mathcal{G}_{LO}\Psi}$, which represents the orbit generated by the action of \mathcal{G}_{LO} on the state $|\Psi\rangle$. The upper panel corresponds to a system of qudits, for which the group of local transformations \mathcal{G}_{LO} is compact. In that case, the Killing two-form is proportional to the identity, adopting the Gell–Mann normalization for $SU(d_\mu)$ generators $T_{(\mu,i)}$ of LOs for the μ th qudits. The lower panel corresponds to a system of harmonic oscillators (qumodes), which in the Gaussian case can be viewed as a non-compact analogue of the qudit system. In this case, the LO group is the symplectic group $Sp(2, \mathbb{R})$, whose Killing two-form is not negative-definite. In panel (c), possible applications of the GEM to the study of multipartite entanglement properties of graph states and discretized scalar fields.

physics have revealed the rich differential geometrical structure of Gaussian states (both for bosons and fermions), clearly illuminating the connection with the theory of Kähler manifolds and generalized group theoretic coherent states [52, 53].

This work expands on the concept of ED to explore multipartite entanglement in multimode bosonic Gaussian states. Specifically, we leverage the geometric framework introduced in a previous study [52] to derive the Gaussian entanglement measure (GEM), a multipartite entanglement monotone extending the concept of ED to pure bosonic Gaussian state manifold (a conceptual scheme is reported in figure 1(a)). Such an extension is non-trivial as it requires a

generalization of the approach adopted in [1] on building a scalar entanglement monotone from the Fubini–Study metric of the Hilbert space restricted to the states that are locally invariant up to LOs. Specifically, this involves extending the procedure for a set of qudits (where the LOs form a compact Lie group) to the case of local Gaussian transformations acting on multimode bosonic Gaussian states, forming a non-compact (semi-simple) Lie group. For providing such an extension, we conveniently reformulate the ED in the language of group-theoretic coherent states and we clarify the close relation between the geometry of the Lie group of LOs and the geometry of the submanifolds of states equivalent up to LOs (see illustrative figure 1(b)). The GEM derived in the current work shares with the ED all the properties characterizing an entanglement measure. In particular, as we will see, the GEM admits a simple analytical expression for every pure Gaussian state in terms of the purities of each part of the considered system. This confers a significant computational advantage, as computing the GEM does not necessitate optimization across the set of separable Gaussian states. Thanks to these features, the GEM is a suitable tool that can be applied to a wide range of systems. Among the possible interesting applications of our results, we treat the case of a bosonic scalar field in two spacetime dimensions. The interplay between quantum information and quantum field theory is a very active area of research, in particular in the framework of holography [54–59]. Traditionally, bipartite entanglement measures such as entanglement entropy have been widely employed to explore the quantum entanglement of quantum fields across two disjoint regions in spacetime. Additionally, our approach to the multipartite entanglement properties of Gaussian states could offer a new quantum information theoretical tool for exploring quantum phase transitions in condensed matter systems. Recent research has highlighted the significance of multipartite entanglement measures linked to quantum Fisher information [27, 60] (as the ED [1]) in gaining deeper insights into many-body correlations [61, 62], thus paving the way toward the comprehension of quantum phase transitions, both in quantum spin systems and in conformal field theory [63]. The paper is structured as follows. In section 1 we will review the definition of the ED introduced in [1] and reformulate it within the framework of group-theoretic coherent state using the geometrical language presented in [52]. We will clarify the introduction of the ED as the scalar invariant obtained by taking the trace of the Fubini–Study metric on the submanifold of states equivalent up to LOs as the contraction with the inverse of the Killing metric defined on the algebra of the LOs group. This reformulation allows us in section 2, in the context of continuous variable Gaussian states, to define and derive an analytical expression for the GEM. We discuss its general properties and how it is related to other known multipartite entanglement measures for Gaussian states. Finally, in section 3 we present the application of the GEM to what we will refer to as *graph state*, and to the ground state of a scalar quantum field theory in two spacetime dimensions (see figure 1(c)). The Conclusion section provides a discussion of how the results obtained in the paper suggest several natural generalizations, possible applications concerning the use of the GEM for better understanding graph-theoretic properties of multimode Gaussian states, as well as for potentially being able to capture topological properties of the spacetime on which a field theory is put.

Notations: Lower case Greek letters denote the mode index. Lower case Latin letters denote Lie algebra indices. Upper case Latin letters denote coordinate indices in phase space.

1. ED from generalized coherent state manifold: general geometric formulation

1.1. Geometry of group-theoretic coherent states

Let us consider a quantum system composed of N subsystems such that the Hilbert space \mathcal{H} of the wavefunctions representing its quantum state can be expressed as the tensor product

of local Hilbert spaces, i.e. $\mathcal{H} = \bigotimes_{i=1}^N \mathcal{H}_i$. The local Hilbert spaces are assumed to all be isomorphic to each other. In the definition of multipartite entanglement monotones, a key role is played by the group of local unitary transformations \mathcal{G}_{LO} , where each element $\hat{U}_{\text{LO}} \in \mathcal{G}_{\text{LO}}$ can be represented as a unitary transformation acting on the Hilbert space \mathcal{H} , taking the form

$$\hat{U}_{\text{LO}} = \hat{I}_1 \otimes \cdots \otimes \hat{U}_i \otimes \cdots \otimes \hat{I}_N \quad (1)$$

for any possible $i = 1, \dots, N$, where \hat{U}_i is a unitary transformation acting on local Hilbert space \mathcal{H}_i . Pure states correspond to rays in \mathcal{H} , namely to normalized vectors up to a global phase. Let us therefore introduce the following equivalence relation:

$$|\Psi\rangle \sim |\Psi'\rangle \iff \exists c \in \mathbb{C}^* \text{ such that } |\Psi\rangle = c|\Psi'\rangle, \quad (2)$$

namely, two vectors are equivalent if they are related through scaling by a non-zero complex number. The space of pure quantum states has then the geometric structure of a projective Hilbert space, i.e. the space of equivalence classes $[|\psi\rangle]$ with respect to the equivalence relation \sim :

$$\mathbb{P}(\mathcal{H}) = (\mathcal{H} \setminus \{\mathbf{0}\}) / \sim. \quad (3)$$

The starting point for defining entanglement monotones is to construct a scalar function of a given quantum state $[|\psi\rangle] \in \mathbb{P}(\mathcal{H})$ that is invariant under local unitary transformations. For this purpose, we adopt the geometric perspective originally introduced by [1], considering a variational manifold $\mathcal{M} \subseteq \mathbb{P}(\mathcal{H})$ of pure quantum states parameterized by a finite set of real parameters $\mathbf{x} \in \mathbb{R}^K$. A comprehensive presentation of such a geometrical framework can be found in [52] and in section I of the supplemental material.

It can be shown that the projective structure of the space of pure quantum states $\mathbb{P}(\mathcal{H})$ and the inner product $\langle \cdot | \cdot \rangle$ defined in the Hilbert space \mathcal{H} induce on the manifold \mathcal{M} a Fubini–Study metric tensor g for each quantum state identified by the coordinates $\mathbf{x} = x^1, \dots, x^K$ of the form

$$g_{AB}([|\psi(\mathbf{x})\rangle]) = 2 \operatorname{Re} \left[\langle \partial_A \psi(\mathbf{x}) | \partial_B \psi(\mathbf{x}) \rangle - \frac{\langle \partial_A \psi(\mathbf{x}) | \psi(\mathbf{x}) \rangle \langle \psi(\mathbf{x}) | \partial_B \psi(\mathbf{x}) \rangle}{\langle \psi(\mathbf{x}) | \psi(\mathbf{x}) \rangle} \right], \quad (4)$$

where $\partial_A = \partial / \partial x^A$ are the partial derivatives with respect to the local patch of coordinates on the manifold \mathcal{M} . In this work, we consider manifolds $\mathcal{M}_{\mathcal{G}\psi_{\text{sep}}}$ generated by the unitary action of a Lie group \mathcal{G} on a separable *seed* state of the form $|\psi_{\text{sep}}\rangle = \bigotimes_{i=1}^N |\phi_i\rangle$ for some $|\phi_i\rangle \in \mathcal{H}_i$, i.e.

$$\mathcal{M}_{\mathcal{G}\psi_{\text{sep}}} = \left\{ \hat{U}(\gamma) |\psi_{\text{sep}}\rangle \in \mathcal{H} \mid \gamma \in \mathcal{G} \right\} / \sim \subset \mathbb{P}(\mathcal{H}) \quad (5)$$

where $\hat{U} : \mathcal{G} \rightarrow U(\mathcal{H})$ is a unitary representation of the Lie group \mathcal{G} on the Hilbert space \mathcal{H} . In particular, let us consider a Lie group \mathcal{G} of dimension $d_{\mathcal{G}}$ and pick a basis $\mathfrak{g} = \operatorname{span}\{T_1, \dots, T_{d_{\mathcal{G}}}\}$ of its Lie algebra \mathfrak{g} . The structure constants c_{AB}^C are defined by:

$$[T_A, T_B] = c_{AB}^C T_C. \quad (6)$$

Moreover, the Lie algebra is endowed with a bilinear symmetric left-invariant form, the Killing form:

$$\kappa_{AB} = \sum_{C,D=1}^{d_{\mathfrak{g}}} c_{AD}^C c_{CB}^D. \quad (7)$$

Through the representation $\widehat{\mathcal{U}}$, it is possible to define a Hermitian operator \widehat{T}_A acting on the Hilbert space \mathcal{H} , associated to the generator T_A :

$$\widehat{T}_A \equiv \left. \frac{d}{ds} \widehat{\mathcal{U}}(e^{isT_A}) \right|_{s=0}. \quad (8)$$

For such a class of variational manifolds, the Fubini–Study metric can be written in terms of the first and second moments of the generators of the Lie algebra \mathfrak{g} in the state $|\psi\rangle$:

$$(g[\psi])_{AB} = -\frac{1}{2} \left\langle \widehat{T}_A \widehat{T}_B + \widehat{T}_B \widehat{T}_A \right\rangle_{\psi} + \left\langle \widehat{T}_A \right\rangle_{\psi} \left\langle \widehat{T}_B \right\rangle_{\psi}, \quad (9)$$

where $\langle \cdot \rangle_{\psi} = \langle \psi | \cdot | \psi \rangle$ is the expectation value in the state $|\psi\rangle$.

For quantifying the multipartite entanglement of a given quantum state $|\phi\rangle \in \mathcal{M}_{\mathcal{G}^{\psi_{\text{sep}}}}$, the entanglement monotones must be invariant under the set of states $\mathcal{M}_{\mathcal{G}_{\text{LO}}\phi}$ generated by a Lie group of LOs $\mathcal{G}_{\text{LO}} \subset \mathcal{G}$, where the corresponding Lie algebra \mathfrak{g}_{LO} is a subalgebra of \mathfrak{g} , i.e. $\mathfrak{g}_{\text{LO}} \subset \mathfrak{g}$. The subalgebra \mathfrak{g}_{LO} can be written as the direct sum of local components $\mathfrak{g}_{\text{LO}} = \bigoplus_{\mu} \mathfrak{h}_{\mu}$, for each of which we pick a basis $\{T_{(\mu,i)}\}_{i=1, \dots, \dim(\mathfrak{h}_{\mu})}$. The Fubini–Study metric induced on the submanifold $\mathcal{M}_{\mathcal{G}_{\text{LO}}\psi}$ can then be expressed as

$$(g[\phi])_{(\mu,i)(\nu,j)} = -\frac{M_{ij}^{\mu\nu} + M_{ji}^{\nu\mu}}{2} + M_i^{\mu} M_j^{\nu}, \quad (10)$$

in terms of the first and second moments of the \mathfrak{g}_{LO} generators in the state $|\phi\rangle$:

$$M_i^{\mu} = \left\langle \widehat{T}_{(\mu,i)} \right\rangle_{\phi}, \quad M_{ij}^{\mu\nu} = \left\langle \widehat{T}_{(\mu,i)} \widehat{T}_{(\nu,j)} \right\rangle_{\phi}. \quad (11)$$

It is worth noting that the diagonal components of the Fubini–Study metric defined in equation (10) are proportional to the quantum Fisher information of the generator $\widehat{T}_{(\mu,i)}$ in the pure state $\rho = |\phi\rangle\langle\phi|$.

1.2. Derivation of entanglement monotones from the geometry of group-theoretic coherent states: the case of ED

Within the geometrical framework introduced above, it is possible to naturally derive invariant scalar quantities over the submanifolds $\mathcal{M}_{\mathcal{G}_{\text{LO}}\phi}$. We revise here the original construction introduced in [1] for the specific case of a system of N d -dimensional qudits. This situation corresponds to the following choice of group of local transformation:

$$\mathcal{G}_{\text{Lo}} = \prod_{\mu=1}^N \text{SU}(d_{\mu}). \quad (12)$$

From the metric tensor in equation (10), a class of functions $f_b : \mathcal{M}_{\mathcal{G}\psi_{\text{sep}}} \rightarrow \mathbb{R}$, invariant under LO transformations, i.e. $f[\mathcal{G}_{\text{LO}}\phi] = f[\phi]$, can be constructed by considering the trace of $g[\phi]$ along both the subsystems and the generator of LO indices. i.e.

$$f_b[\phi] = \sum_{\mu,\nu=1}^N \sum_{i=1}^{n_\mu} \sum_{j=1}^{n_\nu} \left[\delta^{(\mu,i)(\nu,j)} g_{(\mu,i)(\nu,j)} \right] + b \quad (13)$$

where $b \in \mathbb{R}$ is an *a priori* arbitrary parameter. The ED originally introduced in [1] is obtained by fixing the parameter $b \in \mathbb{R}$ such that for a separable state ψ_{sep} the ED is zero, i.e.

$$\text{ED}[\phi] = f_{b_0}[\phi] \quad \text{s.t.} \quad f_{b_0}[\psi_{\text{sep}}] = 0. \quad (14)$$

We remark here that, following [15], the choice for the value of an entanglement monotone on the class of separable state is arbitrary and does not imply any loss of generality in its definition. A detailed geometric interpretation of the ED has been developed in [30]. However for our purpose of extending the ED to Gaussian states, it would be convenient to interpret the ED in the context of a generic Lie group, as presented before. In particular, in the procedure described above for deriving the ED, there is no particular geometrical interpretation in the choice of using the trace of the Fubini–Study metric, i.e. the contraction of the Fubini–Study metric indices over the LO algebra with a Kronecker delta, for defining the \mathcal{G}_{LO} -invariant functions. However, it can be noticed that the Kronecker delta happens to be proportional to the inverse of the Killing form defined on the Lie algebra $\mathfrak{g}_{\text{LO}} = \bigoplus_{\mu=1}^M \mathfrak{su}(d_\mu)$ according to the conventions adopted in [1]. With this interpretation at hand, we propose the following generalized definition of the ED, which then generalizes for every arbitrary Lie algebras \mathfrak{g}_{LO} with Killing form κ is associated

$$\text{ED}_{\mathfrak{g}_{\text{LO}}}[\phi] = a \sum_{\mu,\nu=1}^N \sum_{i=1}^{n_\mu} \sum_{j=1}^{n_\nu} \kappa^{(\mu,i)(\nu,j)} (g[\phi])_{(\mu,i)(\nu,j)} + b, \quad (15)$$

where $a, b \in \mathbb{R}$ are constants that can be fixed to ensure the correct normalization of the entanglement measure; in particular, this generalized ED is non-negative and vanishes for separable states,

$$\text{ED}_{\mathfrak{g}_{\text{LO}}}[\psi_{\text{sep}}] = 0 \quad \text{ED}_{\mathfrak{g}_{\text{LO}}}[\phi] \geq 0. \quad (16)$$

The generalized ED defined in equation (15) reduces to the one in equation (14) for system of qudits in the particular case of $\mathfrak{g}_\mu = \mathfrak{su}(d_\mu)$ for which the Killing form is negative definite.

However, the definition (15) is more generic, and differences with the compact special unitary case relevant for qudits start emerging when the Killing form is non negative definite, i.e. for semi-simple non-compact Lie algebras as in the case of local Gaussian operations acting on a single bosonic mode where the local algebra is given by the real symplectic algebra $\mathfrak{g}_\mu = \mathfrak{sp}(2, \mathbb{R})$. In the next section, we will precisely apply the generalized ED definition presented in equation (15) to multimode bosonic Gaussian states.

2. GEM for pure Gaussian states

In this section we consider the case of a system of bosonic quantum harmonic oscillators (qumodes). The role of the local algebra is then played by the (non-compact) real symplectic algebra $\mathfrak{g}_\mu = \mathfrak{sp}(2, \mathbb{R})$. The projectivized Hilbert space $\mathbb{C}\mathbb{P}^1 = \text{SU}(2)/\text{U}(1)$ (the Bloch sphere)

for a single qubit is indeed naturally replaced by the hyperboloid $\mathbb{H}^1 = \text{Sp}(2, \mathbb{R})/\text{U}(1)$ for a single qumode.

2.1. The geometry of Gaussian states manifold

Let us consider an N -modes bosonic system defined by the algebra of creation annihilation operators

$$\mathcal{A}_N = \left\{ \hat{a}_1, \hat{a}_1^\dagger, \dots, \hat{a}_N, \hat{a}_N^\dagger \right\} \quad (17)$$

satisfying the canonical commutation relation:

$$[\hat{a}_\mu, \hat{a}_\nu^\dagger] = \delta_{\mu\nu}, \quad (18)$$

and the space of pure states belonging to the (projective) Hilbert space $\mathbb{P}(\mathcal{H})$.

It is convenient to introduce the algebra of quadrature operators

$$\{\hat{q}_1, \hat{p}_1, \dots, \hat{q}_N, \hat{p}_N\} = \{\hat{\xi}_1, \dots, \hat{\xi}_{2N}\}, \quad (19)$$

that are related to the creation/annihilation operators by the transformation

$$\hat{a}_\mu = \frac{\hat{q}_\mu + i\hat{p}_\mu}{\sqrt{2}}, \quad \hat{a}_\nu^\dagger = \frac{\hat{q}_\nu - i\hat{p}_\nu}{\sqrt{2}}. \quad (20)$$

and satisfying the commutation relations

$$[\hat{q}_\mu, \hat{p}_\nu] = i\delta_{\mu\nu}. \quad (21)$$

For each state $[|\Psi\rangle] \in \mathbb{P}(\mathcal{H})$, we define the k -point correlation coefficients

$$\mathcal{C}_{A_1, \dots, A_k}([|\Psi\rangle]) = \left\langle \left(\hat{\xi}_{A_1} - \langle \hat{\xi}_{A_1} \rangle_\Psi \right) \dots \left(\hat{\xi}_{A_k} - \langle \hat{\xi}_{A_k} \rangle_\Psi \right) \right\rangle_\Psi. \quad (22)$$

where the capital Latin letters runs over the $2N$ -dimensional phase space, i.e. $A_1, \dots, A_k = 1, \dots, 2N$. In particular, the 2-point correlation coefficients can be rewritten in terms of their symmetric and antisymmetric parts

$$\mathcal{C}_{A,B} = \Gamma_{AB} + \frac{i}{2} \Omega_{AB}, \quad (23)$$

where we have introduced the symmetric tensor

$$\Gamma_{AB} = \frac{1}{2} \left\langle \Psi \left| \left\{ \hat{\xi}_A, \hat{\xi}_B \right\} \right| \Psi \right\rangle = \frac{\mathcal{C}_{AB} + \mathcal{C}_{BA}}{2}, \quad (24)$$

and the anti-symmetric (symplectic) matrix determined by the CCR

$$\Omega_{AB} = -i \left\langle \Psi \left| \left[\hat{\xi}_A, \hat{\xi}_B \right] \right| \Psi \right\rangle = -i(\mathcal{C}_{AB} - \mathcal{C}_{BA}), \quad (25)$$

that, according to our conventions, can be rewritten as

$$\Omega = \bigoplus_{\mu=1}^N \Omega^{(\mu)} = \bigoplus_{\mu=1}^N \begin{pmatrix} 0 & 1 \\ -1 & 0 \end{pmatrix}. \quad (26)$$

In what follows, we will consider the set of Gaussian states parameterized by the matrix Γ such that

$$\langle \xi_A \rangle_{\Gamma} = 0 \text{ for } A = 1, \dots, 2N \quad \text{and} \quad (\Gamma \Omega^{-1})^2 = -\frac{\mathbb{1}}{4}. \quad (27)$$

A property of the Gaussian states as defined in equation (27) is that all the $2n + 1$ -point correlation coefficients vanish while all the $2n$ -point correlation coefficients can be expressed in terms of products of the Γ matrix.

We indicate the generic Gaussian state as $|\Gamma\rangle$, and whenever unambiguous, we will denote by simple brackets the expectation in state $|\Gamma\rangle$.

A remarkable property of the Gaussian states is the well-known Wick theorem: the $2n$ -point functions in state $|\Gamma\rangle$ can be decomposed into the sum of products of 2-point functions

$$\mathcal{C}_{A_1, \dots, A_{2n}}(\Gamma) = \frac{1}{n!} \sum_{\sigma} \mathcal{C}_{A_{\sigma(1)}, A_{\sigma(2)}} \cdots \mathcal{C}_{A_{\sigma(2n-1)}, A_{\sigma(2n)}}, \quad (28)$$

where the sum is over all the permutations of $2n$ elements such that $\sigma(2i - 1) < \sigma(2i)$ for all i .

2.2. Exact computation of the metric tensor: derivation of the GEM

To apply the general definition of the GEM in equation (15) to a multimode pure Gaussian state, it is required to explicitly compute the (non-trivial) metric tensor defined on the Lie subgroup of single-mode LOs discussed above. The other main ingredient is the Killing tensor associated to the algebra of LOs, which is built from copies of the Killing form of $\mathfrak{sp}(2, \mathbb{R})$:

$$\kappa_{ij} = 2 \begin{pmatrix} -1 & 0 & 0 \\ 0 & -1 & 0 \\ 0 & 0 & 1 \end{pmatrix}. \quad (29)$$

We refer the reader to the supplemental material for more information about the metaplectic representation of $\mathfrak{sp}(2, \mathbb{R})$.

The computation of the metric tensor necessitates the estimation of the expectation values expressed in equation (11) for the generators of the algebra of local unitaries and their pairwise products, i.e. 2-points and 4-points functions of the $\hat{q}_{\mu}, \hat{p}_{\mu}$ that can be easily calculated by Wick theorem in equation (28). In the particular case of 4-point functions relevant to us, Wick's theorem gives:

$$\mathcal{C}_{A_1, A_2, A_3, A_4} = \mathcal{C}_{A_1, A_2} \mathcal{C}_{A_3, A_4} + \mathcal{C}_{A_1, A_3} \mathcal{C}_{A_2, A_4} + \mathcal{C}_{A_1, A_4} \mathcal{C}_{A_2, A_3}, \quad (30)$$

while the 2-point function can be expressed in terms of the correlation matrix and the symplectic form as in equation (23) The metric tensor is then obtained by symmetrizing the connected component of the second moments. The reader will find the explicit expression of these moments in the supplemental material. After the dust settles down, we obtain very simple

expressions for the components of the metric tensor $(g[\Gamma])_{(\mu,i)(\nu,j)}$ in terms of the covariance matrix components that we also gather in the supplemental material. Consistently with the notation adopted in section 1.2, the GEM can be defined as

$$\text{GEM}[\Gamma] = \text{ED}_{\oplus_{\mu=1}^N \text{sp}(2,\mathbb{R})}[\Gamma] \quad (31)$$

$$\begin{aligned} &= a \sum_{i,j,\mu,\nu} \kappa^{(\mu,i)(\nu,j)} (g[\Gamma])_{(\mu,i)(\nu,j)} + b \\ &= \frac{a}{8} \sum_{\mu=1}^N \left[\det\left(\Gamma^{(\mu)}\right) - \frac{3}{4} \right] + b, \end{aligned} \quad (32)$$

where the Killing form k is the one defined in equation (29) and the reduced density correlation matrix reads

$$\Gamma^{(\mu)} = \begin{pmatrix} \Gamma_{q_\mu,q_\mu} & \Gamma_{q_\mu,p_\mu} \\ \Gamma_{p_\mu,q_\mu} & \Gamma_{p_\mu,p_\mu} \end{pmatrix}. \quad (33)$$

To fix the normalization parameters a and b , we note that for pure single-mode Gaussian states the equation (27) reads

$$\Gamma^{(\mu)} \left[\Omega^{(\mu)} \right]^{-1} = J^{(\mu)} \quad \text{and} \quad \left[J^{(\mu)} \right]^2 = -\frac{\mathbb{1}}{4}. \quad (34)$$

From the previous definitions, it follows that

$$\begin{aligned} &\left(\Gamma^{(\mu)} \left[\Omega^{(\mu)} \right]^{-1} \right)^2 \\ &= \begin{bmatrix} (\mathcal{C}_{q_\mu,p_\mu} + \mathcal{C}_{p_\mu,q_\mu})^2 - 4\mathcal{C}_{q_\mu,q_\mu}\mathcal{C}_{p_\mu,p_\mu} & 0 \\ 0 & (\mathcal{C}_{q_\mu,p_\mu} + \mathcal{C}_{p_\mu,q_\mu})^2 - 4\mathcal{C}_{q_\mu,q_\mu}\mathcal{C}_{p_\mu,p_\mu} \end{bmatrix} \\ &\stackrel{!}{=} -\mathbb{1}, \end{aligned} \quad (35)$$

from which the following conditions for 2-point functions follow

$$4\mathcal{C}_{q_\mu,q_\mu}\mathcal{C}_{p_\mu,p_\mu} - (\mathcal{C}_{q_\mu,p_\mu} + \mathcal{C}_{p_\mu,q_\mu})^2 = 1, \quad (36)$$

or, equivalently, in terms of the correlation matrix:

$$\Gamma_{p_\mu,q_\mu}^2 = \Gamma_{q_\mu,q_\mu}\Gamma_{p_\mu,p_\mu} - \frac{1}{4}. \quad (37)$$

Therefore, one has for a separable state (setting here $a = 1$)

$$\text{GEM}[\Gamma_{\text{separable}}] = \frac{N}{8} + b. \quad (38)$$

Therefore, setting $a = 1$ and $b = -N/8$ for satisfying the condition on separable states reported in equation (14), the GEM of a pure N -mode Gaussian state is then given by:

$$\text{GEM}[\Gamma] = \frac{1}{8} \sum_{\mu=1}^N \left[\det\left(\Gamma^{(\mu)}\right) - \frac{1}{4} \right]. \quad (39)$$

Let us recall that the purity of a quantum state described by the density matrix ρ is defined as $P(\rho) = \text{tr}(\rho^2)$. For a Gaussian state identified by the covariance matrix Γ , the purity can be simply expressed [64] as:

$$P(\rho) = \frac{1}{2\sqrt{\det(\Gamma)}}. \quad (40)$$

Hence, the GEM can be rewritten in terms of the purities of the subsystems:

$$\text{GEM}[\Gamma] = \frac{1}{32} \sum_{\mu=1}^N \left[\frac{1}{P(\rho^{(\mu)})^2} - 1 \right]. \quad (41)$$

Note that by linearity, one can subtract away the contribution of separable states already at the level of the full metric tensor by defining $h[\Gamma] = g[\Gamma] - g[\Gamma_{\text{separable}}]$, whose explicit expression of the components can be found in the supplemental material. The GEM is then simply given by contraction with the inverse of the Killing metric as before:

$$\begin{aligned} \text{GEM}[\Gamma] &= \sum_{i,j,\mu,\nu} \kappa^{(\mu,i)(\nu,j)} (h[\Gamma])_{(\mu,i)(\nu,j)} \\ &= \frac{1}{32} \sum_{\mu=1}^N \left[\frac{1}{P(\rho^{(\mu)})^2} - 1 \right]. \end{aligned} \quad (42)$$

Let us mention at this point that we could actually choose to normalize the GEM slightly differently, in particular by dividing by a global factor of N , giving the GEM the interpretation of an arithmetic average over the subsystems. We do not choose such a normalization here, but we refer the reader to the end of section 3.2 for another comment about this other possible choice of normalization. It can be very interestingly noticed that another quantity known as the *potential of multipartite entanglement* π_{ME} [65, 66], appears to be defined as an average of the purity over partitions of a quantum state into subsystems, $\pi_{\text{ME}} \propto \sum_{\mu} P(\rho^{(\mu)})$. Our approach can be viewed as providing a first-principles motivation for introducing the average purity of the subsystems. Let us emphasize that the expression can be interpreted as an average over bipartitions where one subsystem consists of a single mode. However, there is no restriction preventing the consideration of more general partitions of the system. For instance, following [65, 66], one could adopt balanced bipartitions, typically used to investigate frustration in states with minimal average purity, by selecting different subalgebras to define the group of LOs \mathcal{G}_{LO} . More generally, our method generates scalar-valued functions on the space of pure Gaussian states that are invariant under a specified group \mathcal{G}_{LO} and are distinct, in principle, from the purity for partitions involving multimode subsystems. In particular, whether our construction could provide new perspectives for solving the problem of the existence of a maximally multipartite state in a system of $N \geq 7$ modes, for which it was observed in [65] that numerical methods scale badly in terms of the parameter space, would constitute an interesting research direction. Finally, we compare GEM with other multipartite entanglement measures for Gaussian states based on the geometric properties of the quantum state space, such as the generalized geometric measure (GGM) [67, 68]. Both GEM and GGM define a distance between states using the Fubini–Study metric, but they differ in approach, particularly for pure-state entanglement. The GGM measures the Fubini–Study distance to the nearest separable state, requiring

a global optimization in Hilbert space. In contrast, GEM inherits from ED the advantage of quantifying separability and multipartite entanglement via the local geometry of the generalized Lie-coherent state manifold generated by unilocal unitary transformations near the given state. Moreover, the two measures adopt different notions of ‘multipartiteness’. Computing the GGM requires considering all possible bipartitions of the system, defining it over an ensemble of partitions. GEM (like ED), instead, quantifies entanglement for a specific partition specified by the Lie subalgebra of local unitary transformations. In this sense, the GEM is a multipartite entanglement monotone; however, it is not a *genuine* measure of multipartite entanglement, as it does not vanish on bipartite separable states [69, 70]. Our geometric approach could potentially offer a means to ensure the genuineness of the constructed measure—either at the level of the Gaussian state manifold or through an appropriate choice of local algebras. The explicit specification of the partition via the subalgebra generating \mathcal{G}_{LO} constitutes a key advantage of the Lie-group generalized coherent-state approach to multipartite entanglement which we will explore further in future work. Such a difference in how we intend the ‘multipartiteness’ also affects scalability for large systems with respect to other methods. For a Gaussian state of N bosonic qumodes, the GGM method requires symplectic diagonalization over all possible bipartitions, resulting in a computational cost of $\mathcal{O}(N^{N/2} \times N^3)$. In contrast, GEM requires only the determinant of a 3×3 matrix for each of the N subsystems, with complexity $\mathcal{O}(3^3 \times N) \sim \mathcal{O}(N)$, thus scaling linearly with system size. We stress that GEM is not the only multipartite entanglement measure that does not involve optimization step (on pure states), but it sits in a large family of entanglement monotones not requiring global optimization see for instance multipartite concurrences [71].

2.3. Properties satisfied by GEM

Generic entanglement measures are required to satisfy axioms [1, 8, 72, 73], that we check below for our GEM measure.

Invariance under local unitaries: This property is natural given the construction. By definition, our quantity only depends on the state up to single-mode unitary transformations.

Positivity: This property is obvious from the expression (41) in terms of the purity.

Upper bound: Due to the non-compactness of $\text{Sp}(2M, \mathbb{R})$, one should not expect our definition to admit an upper bound. We refer the reader to section 3.1.1 below for a comment concerning a possible way to modify the GEM to make it upper-bounded.

Upper bound attained by maximally entangled states: The states playing the role of the maximally entangled Bell states correspond in the continuous variable setting to non-normalizable states of the form $\sum_n |n\rangle \otimes \cdots \otimes |n\rangle$, for which will see in section 3.1.1 that indeed their GEM diverges.

Vanishes on separable states: By using the conditions (14) and (38) we impose that the GEM attains its lower bound at zero for separable states. To be more precise, and in accordance with [74], the GEM of a pure quantum state vanishes if and only if the state is separable.

Non-increasing under Gaussian LOCC: An important property that any entanglement measure should satisfy is that of being non-increasing under the most general operations that are free from the viewpoint of entanglement production. For the ED, which inspired the construction of the GEM, the property of being non-increasing under LOCC has been proven in [30]. In our context, this naturally corresponds to showing that the GEM is non-increasing under Gaussian LOs and classical communication transformations. A detailed proof of this can be found in the Supplemental Material, thereby justifying the designation of the GEM as an *entanglement monotone*.

2.4. Extension to mixed Gaussian state

The GEM, which relies on the Fubini–Study metric restricted to the Gaussian state manifold, is defined for pure Gaussian states in analogy with its precursor, the ED. However, it is possible to naturally extend the GEM to mixed Gaussian states following the convex roof construction, similar to what has been proposed for the ED.

In particular, using well-known properties of the decomposition of mixed Gaussian states $\rho(\Gamma, 0)$ into pure Gaussian states $\rho(\Gamma_p, \mathbf{d})$, which depend on a displacement vector $\mathbf{d} - \mathbf{r}$ and a correlation matrix $\Gamma_p \leq \Gamma$ -i.e. such that $\Gamma - \Gamma_p$ is semi-positive definite [47, 75]-we obtain

$$\rho(\Gamma, 0) \propto \int \rho(\Gamma_p, \mathbf{d} - \mathbf{r}) e^{-\frac{1}{2} \mathbf{r}^T (\Gamma - \Gamma_p)^{-1} \mathbf{r}} d^N \mathbf{r}. \quad (43)$$

This provides a convex decomposition of any arbitrary mixed state into pure Gaussian states. Since the displacement vector $\mathbf{d} - \mathbf{r}$ does not contribute to the GEM, it is straightforward to define the convex roof of the GEM as

$$\text{GEM}[\rho(\Gamma, \mathbf{d})] = \inf_{\Gamma_p \leq \Gamma} \text{GEM}[\Gamma_p]. \quad (44)$$

3. Examples

Generic families of multimode Gaussian states are obtained using Hermitian Hamiltonians that are quadratic in the quadratures, or in the creation and annihilation operators. If we define multimode generators generalizing their single-mode counterpart as follows:

$$\begin{aligned} \hat{T}_{1,\mu\nu} &= \frac{\hat{a}_\mu \hat{a}_\nu + \hat{a}_\mu^\dagger \hat{a}_\nu^\dagger}{4}, & \hat{T}_{2,\mu\nu} &= -\frac{\hat{a}_\mu \hat{a}_\nu - \hat{a}_\mu^\dagger \hat{a}_\nu^\dagger}{4i}, \\ \hat{T}_{3,\mu\nu} &= \frac{\hat{a}_\mu^\dagger \hat{a}_\nu + \hat{a}_\mu \hat{a}_\nu^\dagger}{4}, & \hat{T}_{4,\mu\nu} &= -\frac{\hat{a}_\mu^\dagger \hat{a}_\nu - \hat{a}_\mu \hat{a}_\nu^\dagger}{4i}, \end{aligned} \quad (45)$$

one can indeed define the following families of N -mode Gaussian states:

$$|\{c_{i,\mu\nu}\}\rangle = U(\{c_{i,\mu\nu}\}) |0\rangle = e^{i\hat{H}(\{c_{i,\mu\nu}\})} |0\rangle \quad (46)$$

with the following generic Hermitian generator:

$$\hat{H}(\{c_{i,\mu\nu}\}) = \sum_{\mu,\nu=1}^N \sum_{i=1}^4 c_{i,\mu\nu} \hat{T}_{i,\mu\nu}, \quad (47)$$

and real coefficients $c_{i,\mu\nu}$. For a given number of modes N , this family of states is $N(2N + 1)$ -dimensional, which is of course the dimension of the symplectic algebra $\mathfrak{sp}(2N, \mathbb{R})$.

For visualization, we will illustrate the GEM for low dimensional sub-families of states which we will refer to as *graph states* in what follows. In this work, we restrict our analysis to the analytic expression of GEM graph states with at most three states. However, nothing prevents extending the study to more complex graph states with additional nodes, whose computational cost would scale linearly with the number of nodes (see section 2.2 for more details).

We also study the case of a massive Klein–Gordon field in two spacetime dimensions to illustrate the applicability of our results to systems with a large number of degrees of freedom.

3.1. Graph states

Hence, let us introduce a family of multimode Gaussian states obtained by setting $c_{1,\mu\nu} = c_{4,\mu\nu} = 0$ in equation (47). We also set by convention the remaining variables to

$$c_{3,\mu\nu} = 4 \operatorname{Re}(A_{\mu\nu}), \quad c_{2,\mu\nu} = 4 \operatorname{Im}(A_{\mu\nu}), \quad (48)$$

and $A_{\mu\nu} = 0$ if $\mu = \nu$. The states are then parameterized by the set of complex numbers $\{A_{\mu\nu}\}$ and given by

$$|\psi\rangle = U(\{A_{\mu\nu}\}) |0\rangle, \quad (49)$$

with

$$U(\{A_{\mu\nu}\}) = \exp \left[i \sum_{\substack{\mu, \nu=1 \\ (\mu < \nu)}}^N (\operatorname{Re}(A_{\mu\nu}) \hat{a}_\mu^\dagger \hat{a}_\nu + i \operatorname{Im}(A_{\mu\nu}) \hat{a}_\mu \hat{a}_\nu + \text{h.c.}) \right]. \quad (50)$$

The unitary operator generating this N -mode state can be expressed in quadrature basis as

$$U(\{A_{\mu\nu}\}) = \exp \left[\frac{i}{2} \hat{\xi}^T h(\{A_{\mu\nu}\}) \hat{\xi} \right], \quad (51)$$

with the $h(\{A_{\mu\nu}\})$ matrix being built out of blocks

$$q_\mu \begin{pmatrix} q_\nu & p_\nu \\ \operatorname{Re}(A_{\mu\nu}) & -\operatorname{Im}(A_{\mu\nu}) \end{pmatrix}, \quad p_\mu \begin{pmatrix} -\operatorname{Im}(A_{\mu\nu}) & \operatorname{Re}(A_{\mu\nu}) \end{pmatrix}, \quad (52)$$

when $\mu \neq \nu$, and the trivial matrix $\mathbf{0}_2$ if $\mu = \nu$. The corresponding symplectic transformation then reads:

$$S(\{A_{\mu\nu}\}) = \exp[\Omega h(\{A_{\mu\nu}\})]. \quad (53)$$

The covariance matrix is then given by

$$\Gamma(\{A_{\mu\nu}\}) = \frac{1}{2} S(\{A_{\mu\nu}\}) S(\{A_{\mu\nu}\})^T \quad (54)$$

The coupling constants $\{A_{\mu\nu}\}$ are naturally interpreted as the complex weights carried by the edges of a graph connecting the N modes. In what follows, we will treat the case of $N = 2$ and $N = 3$ node graphs.

3.1.1. Two-mode states. In the particular case of a two-mode state, we denote by $w = A_{12}$ the single coupling appearing in the Hamiltonian. The GEM can be computed exactly as a function of w :

$$\text{GEM}[|w\rangle] = \frac{\operatorname{Im}(w)^2 \sin^2 \left(2\sqrt{\operatorname{Re}(w)^2 - \operatorname{Im}(w)^2} \right)}{16 \left(\operatorname{Re}(w)^2 - \operatorname{Im}(w)^2 \right)}. \quad (55)$$

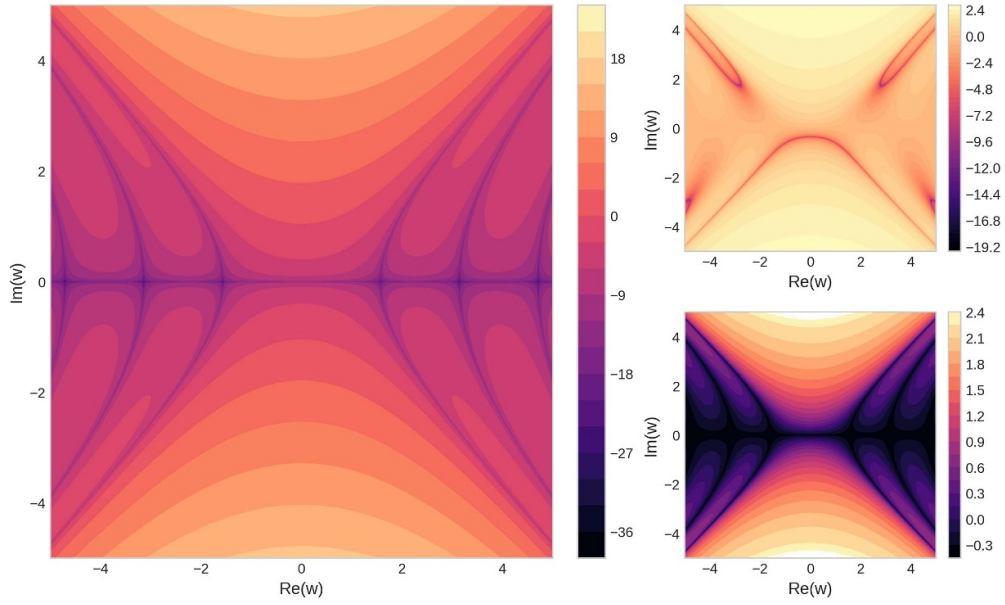


Figure 2. Comparison of our GEM with other well-known measures of entanglement for the two-mode graph states. Left: logarithm of the geometric Gaussian entanglement measure. Top right: logarithm of the entanglement of formation. Bottom right: logarithm of the logarithmic negativity.

We refer the reader to figure 2 (on the left) for a depiction of the GEM as a function of the complex coupling w . Two other well-known measures of entanglement for bipartite quantum states are depicted in the same figure: the entanglement of formation [76–78] (computed using the algorithm of [79]) and the logarithmic negativity [80]. We observe that the GEM behaves qualitatively like these to other measures. Let us recall that the entanglement of formation is notoriously difficult to compute in general, being the solution to a complex optimization problem.

By expressing the complex coupling w in polar coordinates as $w = re^{i\phi}$, one can reexpress the GEM (55) as follows:

$$\text{GEM}[|w\rangle] = \frac{\sin^2(\phi) \sin^2\left(2r\sqrt{\cos(2\phi)}\right)}{16 \cos(2\phi)}. \quad (56)$$

An interesting feature appears in the large squeezing limit. Let us set, for a moment, $\phi = \pm\pi/2$ to turn off the pure beamsplitter component and focus on the two-mode squeezing contribution. In that case, the GEM reduces to:

$$\text{GEM}[|w\rangle] = \frac{1}{16} \sinh^2(2r). \quad (57)$$

One can show [81] that the Schmidt decomposition (over Fock states) of the two-mode squeezed state reads:

$$\exp\left[r\left(a_1^\dagger a_2^\dagger - a_1 a_2\right)\right] |0\rangle = \frac{1}{\cosh(r)} \sum_{i \geq 0} \tanh^i(r) |i\rangle \otimes |i\rangle. \quad (58)$$

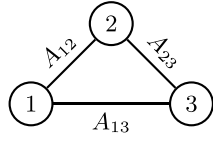


Figure 3. Generic complex coupling coefficients.

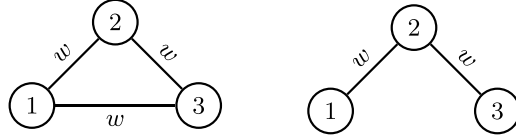


Figure 4. First family of three-mode graph states, with identical complex couplings.

In particular, in the limit of large squeezing $r \rightarrow \infty$, this state converges to the balanced superposition of all the states of the form $|i\rangle \otimes |i\rangle$. Though non-normalizable, this state, similarly to EPR states for qubits, corresponds to a maximally entangled state. Once again, this is consistent with the fact that the GEM diverges in the infinite squeezing limit. This observation hints towards a possible new definition of a compact GEM that is, in this case, bounded from above by the entanglement measure of such non-normalizable EPR-like states. Such an upper bound of the entanglement measure can be set to 1 by convention. For this two-mode example in particular, this can be achieved by bounding the values that the modulus of w can take by substituting, for instance, $r = \tanh(\nu)$, and by normalizing the GEM as follows:

$$\text{GEM} [|\tanh(\nu) e^{i\phi}\rangle] = \frac{1}{2 \sinh^2(2)} \left[\frac{1}{P(\rho^{(1)})^2} + \frac{1}{P(\rho^{(2)})^2} - 2 \right]. \quad (59)$$

The GEM is then bounded from above by 1. This regularization can be viewed as effectively compactifying the space of Gaussian states by constraining the possible energy of the states [82, 83] (with respect to a Hamiltonian $\sum_{\mu} \frac{p_{\mu}^2 + q_{\mu}^2}{2}$).

Finally, it can be noticed that the full metric tensor can be computed exactly, as can be seen by the interested reader in the supplemental material.

3.1.2. Three-mode states. In the case of a three-mode state, one can consider two different (connected) graph topologies. Each edge carries a complex weight (cf figure 3); therefore, the family of states is six-dimensional. To visualize the GEM, we reduce the study to two separate two-dimensional families of states.

First family:

For the first family of states, we set all the non-zero complex couplings to be identical, and we consider both the fully connected graph (G1), and the graph with one edge turned off (G2), cf figure 4.

The GEM can be expressed explicitly. For G1 we obtain:

$$\begin{aligned} \text{GEM}_{\text{G1}}(w) &= \frac{\text{Im}(w)^2 \sin^2 \left(3\sqrt{\text{Re}(w)^2 - \text{Im}(w)^2} \right)}{12 \left(\text{Re}(w)^2 - \text{Im}(w)^2 \right)} \\ &= \frac{1}{12} \sin^2(\phi) \sec(2\phi) \sin^2 \left(3r\sqrt{\cos(2\phi)} \right), \end{aligned} \quad (60)$$

and for G2:

$$\begin{aligned} \text{GEM}_{\text{G2}}(w) &= \frac{\text{Im}(w)^2 \sin^2 \left(\sqrt{2}\sqrt{\text{Re}(w)^2 - \text{Im}(w)^2} \right) \left(3 \cos \left(2\sqrt{2}\sqrt{\text{Re}(w)^2 - \text{Im}(w)^2} \right) + 5 \right)}{32 \left(\text{Re}(w)^2 - \text{Im}(w)^2 \right)} \\ &= \frac{1}{32} \sin^2(\phi) \sec(2\phi) \sin^2 \left(r\sqrt{\sin(4\phi) \csc(2\phi)} \right) \left(3 \cos \left(2r\sqrt{\sin(4\phi) \csc(2\phi)} \right) + 5 \right). \end{aligned} \quad (61)$$

Note that the full metric tensor can be computed for both graphs and is provided for completeness in the supplemental material.

In figure 5 we depict the logarithm of the GEM for these two cases, as well as the ratio of the GEM of graph 2 and graph 1. The first observation concerns the fact that a purely real coupling does not generate entanglement. To proceed with interpreting the results, it is fruitful to consider the graph weights to be all proportional to a common time parameter t . Therefore, an increase in the amplitude of the couplings corresponds to time evolution. Within this picture, the state preparation provided in equation (49) can naturally be interpreted as the unitary time evolution given by equation (49) of an initial state corresponding to the tensor product of Fock vacua under. Equipped with this interpretation, the comparison of the GEM for the two graph topologies becomes clear and compatible with a first intuition: the fully connected graph allows for a faster entanglement. However, for long times, the two GEM become identical, as can be seen in figure 4 (on the right), indicating that the logarithm of their ratio tends to zero for large amplitudes of w .

Interestingly, we note that the ratio

$$\begin{aligned} \frac{\text{GEM}_{\text{G2}}}{\text{GEM}_{\text{G1}}}(w) &= \frac{3 \sin^2 \left(\sqrt{2}\sqrt{\text{Re}(w)^2 - \text{Im}(w)^2} \right)}{8 \sin^2 \left(3\sqrt{\text{Re}(w)^2 - \text{Im}(w)^2} \right)} \\ &\quad \times \left(3 \cos \left(2\sqrt{2}\sqrt{\text{Re}(w)^2 - \text{Im}(w)^2} \right) + 5 \right) \\ &= \frac{3}{8} \csc^2 \left(3r\sqrt{\cos(2\phi)} \right) \sin^2 \left(r\sqrt{\sin(4\phi) \csc(2\phi)} \right) \\ &\quad \times \left(3 \cos \left(2r\sqrt{\sin(4\phi) \csc(2\phi)} \right) + 5 \right), \end{aligned} \quad (62)$$

has the following finite limit on the two principal axes in the w complex plane, corresponding to $\phi \rightarrow \frac{\pi}{4} + \frac{n\pi}{2}$ with $n \in \{0, 1, 2, 3\}$ (or $r \rightarrow 0$):

$$\frac{\text{GEM}_{\text{G2}}}{\text{GEM}_{\text{G1}}} \rightarrow \frac{2}{3}, \quad (63)$$

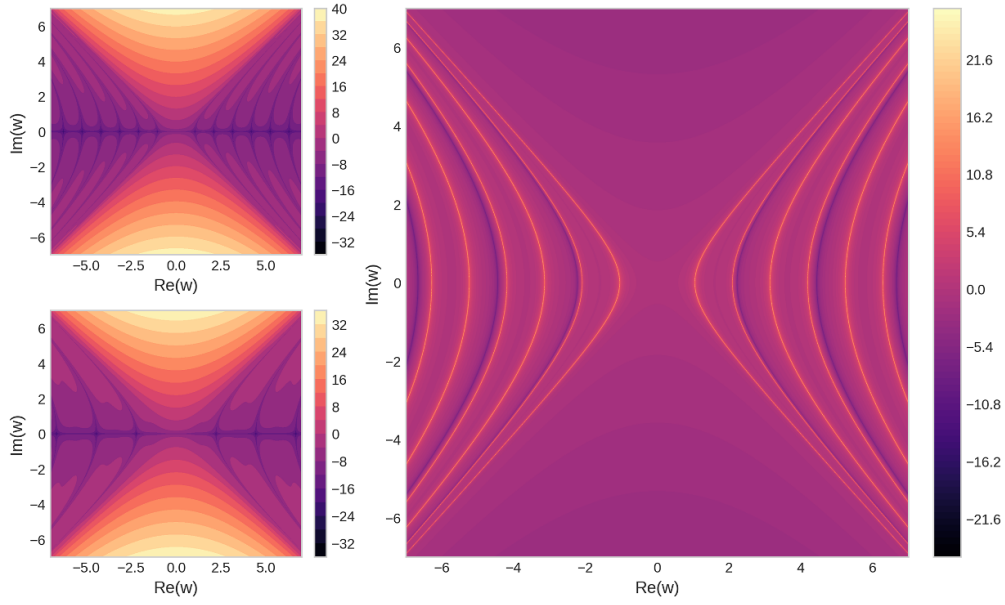


Figure 5. GEM for the first family of three-mode graph states. Top left: logarithm of the GEM for the fully connected graph. Bottom left: logarithm of the GEM for the partially connected graph. Right: logarithm of the ratio of the partially connected GEM to the fully connected GEM.

which is precisely the ratio of the number of edges in the two graphs.

Let us mention, without entering into the details, that the above observation concerning how the ratio of GEMs captures information about the connectivity of the underlying graphs actually generalizes to more complicated graph topologies, as can be seen when inspecting the ratio of GEMs for 4-mode graph states (with obvious notations):

$$\begin{aligned}
 \frac{\text{GEM}(\square)}{\text{GEM}(\boxtimes)} &\rightarrow \frac{5}{6}, & \frac{\text{GEM}(\square)}{\text{GEM}(\boxtimes)} &\rightarrow \frac{2}{3}, \\
 \frac{\text{GEM}(\sqcup)}{\text{GEM}(\sqcup)} &\rightarrow \frac{2}{3}, & \frac{\text{GEM}(\sqcup)}{\text{GEM}(\square)} &\rightarrow \frac{2}{5}, \\
 \frac{\text{GEM}(\sqcup)}{\text{GEM}(\square)} &\rightarrow \frac{1}{2}, & \frac{\text{GEM}(\square)}{\text{GEM}(\square)} &\rightarrow \frac{4}{5}.
 \end{aligned} \tag{64}$$

Second family: Given that, as we saw, the real part of the coupling does not play an important role regarding the generation of entanglement in the sense of our measure, and in order to study the effect of the ratio of the communication strength between the vertices of the graph, let us now set $\text{Re}(A_{\mu\nu}) = 0$ and consider again the two graph topologies discussed above.

Indeed, as observed on figures 2 and 5, and consistently with other measures of multipartite entanglement, the real part of the coupling coefficients does not generate entanglement *conditioned on the imaginary part of the couplings being 0*. The reason can be understood in both

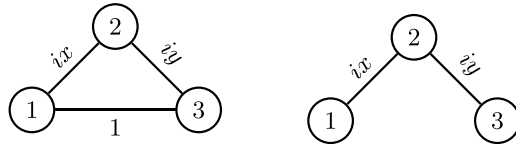


Figure 6. Second family of three-mode graph states, with imaginary unequal couplings.

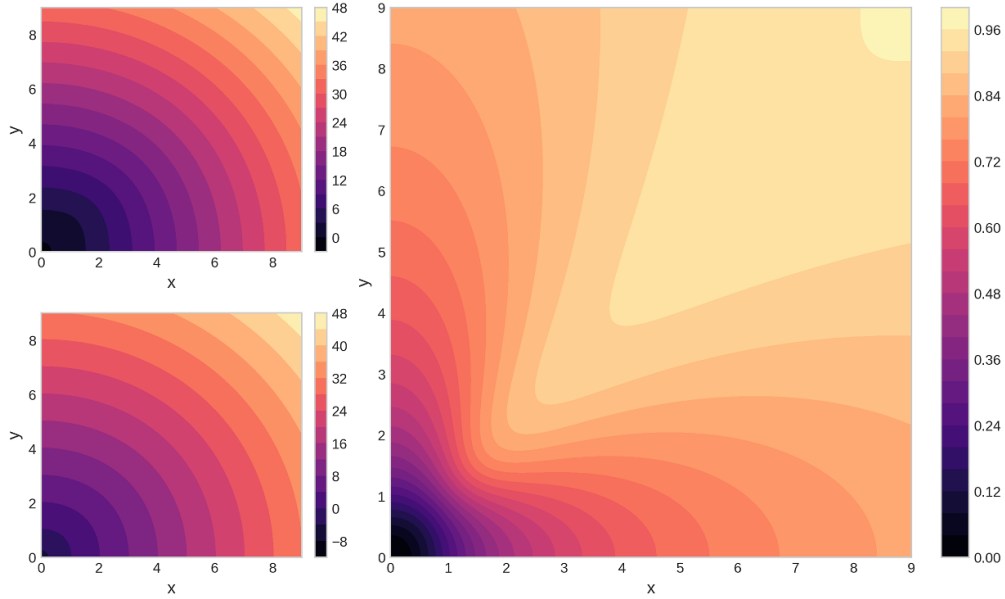


Figure 7. GEM for the second family of three-mode graph states. Top left: logarithm of the GEM for the fully connected graph. Bottom left: logarithm of the GEM for the partially connected graph. Right: ratio of the partially connected GEM to the fully connected GEM.

an algebraic and geometric way. The algebraic way is the following: the purely real part corresponds to a two-mode beam-splitter contribution, that, when fed a zero-photon state, outputs a zero-photon state. Using the ‘geometry of the variational method’ framework from section 1 of the Supplementary Information, we find that, geometrically, the tangent vector in Hilbert space, $|V_{T_{3,\mu\nu}}|0\rangle$, at the ground state associated with the generator $\hat{T}_{3,\mu\nu}$ of unitary Bogoliubov transformations, is null—that is, $|V_{T_{3,\mu\nu}}|0\rangle = 0$.

For the fully connected graph (G1) we set $A_{13} = 1$, and for both graphs we set $A_{12} = ix$ and $A_{23} = iy$, cf figure 6. Inspecting the ratio of the GEMs, reported in figure 7, we observe that asymptotically at large times (or large strength of the couplings), the ratio tends to 1. Namely provided enough time has passed, the two states reach the same level of entanglement in the sense of our measure. However, we observe that the more balanced the strength x and y of the two edges are, the faster the two states reach a similar level of GEM entanglement.

3.2. Free scalar field

Instead of considering systems with slightly more degrees of freedom, let us directly study the case of a very large number of bosonic modes. We therefore consider in this section a massive real Klein–Gordon field in $(1 + 1)$ dimensions (we set the speed of light c to unity). We refer the reader to the supplemental material for details concerning this example.

We compactify the spatial dimension on a circle S^1 of radius R . The Lagrangian density of the system reads (we use the signature $(+, -)$ for the flat Lorentzian metric):

$$\mathcal{L} = \frac{1}{2} (\partial_\mu \phi \partial^\mu \phi - m^2 \phi^2). \quad (65)$$

Introducing, as usual, the conjugate momentum to the field

$$\Pi = \frac{\partial \mathcal{L}}{\partial (\partial_0 \phi)} = \partial_0 \phi, \quad (66)$$

the Hamiltonian density reads:

$$\mathcal{H} = \frac{1}{2} (\Pi^2 + (\nabla \phi)^2 + m^2 \phi^2). \quad (67)$$

We discretize the theory and solely consider the values of the field and its conjugate momentum on a lattice $\mathbb{Z}_N \subset S^1$ composed of $N = 2n + 1$ points $\{x_\mu\}_{\mu=1}^N$ separated by a distance $\delta = 2\pi R/N$. The discretized Hamiltonian can be diagonalized by discrete Fourier transform, giving rise to normal modes of frequencies:

$$\omega_k = \sqrt{m^2 + \frac{4}{\delta^2} \sin^2 \left(\frac{\pi k}{N} \right)}. \quad (68)$$

The ground state $|\emptyset\rangle$ can then be obtained from a Bogoliubov transformation [84]. All the details of the derivation can be found in the supplemental material. After all dust settles down, we obtain the following expression for the GEM of the ground state of the discretize QFT:

$$\text{GEM} [|\emptyset\rangle] = \frac{1}{32N} \left[1 + 2 \sum_{k=1}^{\frac{N-1}{2}} \left(\frac{m}{\omega_k} + \frac{\omega_k}{m} \right) + 4 \sum_{k=1}^{\frac{N-1}{2}} \sum_{k'=1}^{\frac{N-1}{2}} \frac{\omega_k}{\omega_{k'}} \right] - \frac{N}{32}. \quad (69)$$

In the large mass limit, the GEM vanishes

$$\text{GEM} [|\emptyset\rangle] \xrightarrow{m \rightarrow \infty} 0, \quad (70)$$

which is consistent with the fact that in the infinite mass limit, the coupling between neighboring sites becomes subleading, and therefore quantum correlations are not present in the vacuum state, which simply corresponds to the (separable) tensor product of single site states. Instead, in the limit of small mass parameter, the GEM diverges as the inverse of the mass:

$$\text{GEM} [|\emptyset\rangle] \underset{m \rightarrow 0}{\sim} \frac{1}{32\pi Rm} \cot \left(\frac{\pi}{2N} \right). \quad (71)$$

This is also consistent with the fact that the continuum theory becomes conformal in that limit because of the absence of any typical length scale.

Another very interesting limit is the continuum limit, in which the regularization parameter $N = 2n + 1$ goes to infinity for fixed mass m and radius of space R . In the supplemental material, we derive the asymptotic behavior of the GEM at large n . We obtain the following behavior:

$$\text{GEM}[[\emptyset]] \underset{n \rightarrow \infty}{\sim} \kappa_p^{(1)}(\tau) + \kappa_p^{(2)}(\tau) \log n + \kappa_p^{(3)}(\tau) n + \kappa_p^{(4)}(\tau) n \log n + \mathcal{O}(n^2),$$

where $\tau = mR$, and where the parameter $p \in \mathbb{N}$, the ‘Bernoulli cutoff’, is explained in the supplemental material. Let us simply say that, in principle, the larger the cutoff, the more precise the value of the coefficients $\kappa_p^{(\ell)}(\tau)$, but that in practice the *a priori* very crude approximation $p = 0$ already gives a very good estimate. Therefore we observe that the GEM diverges in the limit of an infinitely dense lattice in a controlled way. A few comments should be made at this point. First, note that the coefficients $\kappa_p^{(\ell)}$ depend on the mass and radius only through their dimensionless combination τ . Second, the coefficients $\kappa_p^{(2)}$ and $\kappa_p^{(4)}$ turn out to depend neither on the Bernoulli cutoff p , nor on the modulus τ . They are given by

$$\kappa_p^{(2)}(\tau) = \frac{1}{16\pi}, \quad \kappa_p^{(4)}(\tau) = \frac{1}{4\pi^2}. \tag{73}$$

Euler–Maclaurin expansions generally give good approximations already for small values of the Bernoulli cutoff, and this is indeed what we observe when plugging in some dummy values of the modulus, like $\tau = 1$. We observe a stabilization of $\kappa_p^{(1)}$ and $\kappa_p^{(3)}$ already for $p = 3$, and actually $p = 0$ is already converged at two decimal figures. We report here the analytical expression of the running coefficients for $p = 0$ and $p = 1$ in the supplemental material.

Note that one can directly check that the asymptotic behavior given in equation (72) is perfectly correct, as can be seen in figure 8.

Finally, let us say that had we chosen to normalize our expression of the GEM (41) with an extra factor scaling linearly in the size of the system, the above asymptotic behavior would be slightly simpler, and reduce to the following universal behavior:

$$\text{GEM}[[\emptyset]] \underset{N \rightarrow \infty}{\sim} \frac{1}{4\pi^2} \log N + \mathcal{O}(1). \tag{74}$$

This choice of normalization, whose motivation *a posteriori* originates from these continuum/large volume limit considerations, could be interpreted as a GEM per mode, a GEM density. Note in particular from (74) the absence of dependence on the mass parameter m , which in light of equation (70) shows the non-commutativity of the large mass and continuum limits.

4. Outlook

In this work, we have defined the GEM, a simple scalar measure of quantum correlations in multimode Gaussian states. The intuition is rooted in the geometric description of the space of Gaussian states [52], leveraging the Riemannian metric and action of the local Gaussian unitary transformations, in the spirit of what was done for discrete systems in [1, 30]. We then computed the GEM for various natural families of Gaussian states and observed, in particular, in the multimode graph case, that it naturally captures some topological properties of the underlying graph defining the state.

Let us mention a few natural directions suggested by our definition. Our work naturally extends the results of [1] and can be viewed as a non-compact version of their qubit examples,

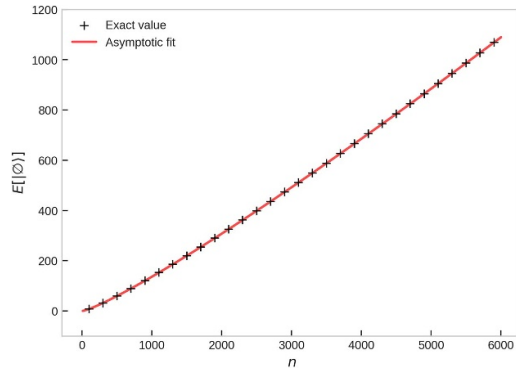


Figure 8. Asymptotic fit of the GEM of the free massive Klein–Gordon field, with mass $m = 1$ and radius of space $R = 1$. We observe a perfect agreement between the exact result given by equation (69) and the asymptotic behavior predicted by equation (72).

for which the local algebra of unitaries $\bigoplus_{\mu} \mathfrak{su}(2) \in \mathfrak{su}(2^N)$ is naturally replaced by the symplectic group $\bigoplus_{\mu} \mathfrak{sp}(2, \mathbb{R}) \in \mathfrak{sp}(2N, \mathbb{R})$. From a geometric perspective, this leads to structures reminiscent of the well-known Segre embedding for qubit systems [85], but where the Bloch sphere $\mathbb{C}\mathbb{P}^1 = \text{SU}(2)/\text{U}(1)$ is now replaced by the hyperboloid $\mathbb{H}^1 = \text{SU}(1, 1)/\text{U}(1)$. More generally, the freedom in the choice of the algebra of local transformations allows for a broad generalization of our definition. Given an N -mode system, one can consider the set of partitions of the set of modes. Given a partition P , one associates to it the subalgebra $\bigoplus_{\sigma \in P} \mathfrak{sp}(2|\sigma|, \mathbb{R}) \in \mathfrak{sp}(2M, \mathbb{R})$, which can then be chosen as the algebra of *local* transformations. The choice made in this paper corresponds to the choice of the finest partition of the set of modes. The set of partitions is naturally endowed with a partial order corresponding to the level of refinement, and we would expect our GEM to respect that partial order, in the sense that given a state $|\psi\rangle$, its GEM for the coarsest partition (containing solely the whole set of modes) should vanish identically, and should be non-decreasing as the partition is being refined, reaching a maximal value for the finest partition described in this paper. This is left for future investigations.

We saw that the GEM can naturally be expressed in terms of a quadratic Casimir, namely a quadratic element of the center of the universal enveloping algebra. Though slightly deviating from the geometric root of our definition, this observation naturally suggests the possibility of defining a family of entanglement measures in terms of higher-order Casimir operators.

Gaussian states represent an extremely rich class of continuous variable quantum states. However, including even richer families of states beyond Gaussianity is of critical importance. One possibility consists in considering the stellar representation of quantum states, which provides a neat framework in which non-Gaussianities can be implemented in a very controlled way in terms of the *stellar rank* [86] (number of zeros of the Husimi Q -function in phase space). Another approach could be to consider families of states generated by the action of higher-order Hamiltonian, as described in [87]. Yet another extension could be to finite linear combinations of Gaussian states, a prototypical example being that of Schrödinger cat states. In the same way that the so-called ‘Gaussian mixture models’ provide accurate approximations of arbitrary complex (hence non-Gaussian) probability density measures, one can expect that complex quantum states can be approximated arbitrarily well by linear combination of Gaussian states. Combined with a ‘quantum Gaussian mixture model’ algorithm (cf

for instance [88] for a possible approach), this could provide a possible interesting avenue for defining accurate entanglement measures for non-Gaussian states.

Regarding the potential application of the GEM to mixed Gaussian states, we have explored its possible extension through the canonical convex roof construction, in analogy with the extension of the ED to mixed states [1, 29]. However, the intricate mathematical structure of Gaussian states allows for alternative approaches for extending the GEM to mixed Gaussian states. For instance, a mixed Gaussian state characterized by the density matrix ρ_{mix} for a set \mathcal{A} of N bosonic modes can be associated, via the thermofield double construction, with an extended system comprising an additional set of N bosonic modes, denoted as \mathcal{A}' . This leads to a pure Gaussian state $\rho_{\mathcal{A}\mathcal{A}'}$ such that $\text{Tr}_{\mathcal{A}'} \rho_{\mathcal{A}\mathcal{A}'} = \rho_{\text{mix}}$. Within this framework, a natural extension of the GEM for mixed Gaussian states could be defined in terms of the GEM of the corresponding pure thermofield double Gaussian state. Finally, it will be of great interest to consider the case of bosonic field theories in higher dimension, for instance, a free boson on $\mathbb{R}_t \times \Sigma_g$, where Σ_g is a compact Riemann surface of genus g . Generally, the coefficients appearing in the asymptotic expansion obtained when switching off the UV cutoff of the theory could capture some invariants of the underlying manifold.

Data availability statement

The Wolfram Mathematica and Python scripts used to generate the primary data underlying figures 2, 5, 7, and 8 are available from the corresponding author upon reasonable request.

Supplementary data available at <https://doi.org/10.1088/1751-8121/ae21a9/data1>.

Acknowledgments

The authors acknowledge funding via the FNR-CORE Grant ‘BroadApp’ (FNR-CORE C20/MS/14769845) and ERC-AdG Grant ‘FITMOL’.

Conflicts of interests

The Authors declare no Competing Financial or Non-Financial Interests.

ORCID iD

Matteo Gori  0000-0002-0777-133X

References

- [1] Cocchiarella D, Scali S, Ribisi S, Nardi B, Bel-Hadj-Aissa G and Franzosi R 2020 Entanglement distance for arbitrary M -qudit hybrid systems *Phys. Rev. A* **101** 042129
- [2] Arya F *et al* 2019 Quantum supremacy using a programmable superconducting processor *Nature* **574** 505
- [3] Wu Y *et al* 2021 Strong quantum computational advantage using a superconducting quantum processor *Phys. Rev. Lett.* **127** 180501
- [4] Ma W-L, Puri S, Schoelkopf R J, Devoret M H, Girvin S M and Jiang L 2021 Quantum control of bosonic modes with superconducting circuits *Sci. Bull.* **66** 1789
- [5] Tebbenjohanns F, Mattana M L, Rossi M, Frimmer M and Novotny L 2021 Quantum control of a nanoparticle optically levitated in cryogenic free space *Nature* **595** 378
- [6] Vidal G and Tarrach R 1999 Robustness of entanglement *Phys. Rev. A* **59** 141

- [7] Vidal G 2000 Entanglement monotones *J. Mod. Opt.* **47** 355
- [8] Vedral V, Plenio M B, Rippin M A and Knight P L 1997 Quantifying entanglement *Phys. Rev. Lett.* **78** 2275
- [9] Horodecki M, Horodecki P and Horodecki R 2000 Limits for entanglement measures *Phys. Rev. Lett.* **84** 2014
- [10] Eisert J, Simon C and Plenio M B 2002 On the quantification of entanglement in infinite-dimensional quantum systems *Phys. A. Math. Gen.* **35** 3911
- [11] Plenio M B and Virmani S 2007 An introduction to entanglement measures *Quantum Inf. Comput.* **7** 1–51
- [12] Lancien C, Di Martino S, Huber M, Piani M, Adesso G and Winter A 2016 Should entanglement measures be monogamous or faithful? *Phys. Rev. Lett.* **117** 060501
- [13] Bennett C H, DiVincenzo D P, Smolin J A and Wootters W K 1996 Mixed-state entanglement and quantum error correction *Phys. Rev. A* **54** 3824
- [14] Popescu S and Rohrlich D 1997 Thermodynamics and the measure of entanglement *Phys. Rev. A* **56** R3319
- [15] Vidal G 1999 Entanglement of pure states for a single copy *Phys. Rev. Lett.* **83** 1046
- [16] Wootters W K 1998 Entanglement of formation of an arbitrary state of two qubits *Phys. Rev. Lett.* **80** 2245
- [17] Bennett C H, Brassard G, Popescu S, Schumacher B, Smolin J A and Wootters W K 1996 Purification of noisy entanglement and faithful teleportation via noisy channels *Phys. Rev. Lett.* **76** 722
- [18] Horodecki M, Horodecki P and Horodecki R 1998 Mixed-state entanglement and distillation: Is there a ‘bound’ entanglement in nature? *Phys. Rev. Lett.* **80** 5239
- [19] Shimony A 1995 Degree of entanglement *Ann. N. Y. Acad. Sci.* **755** 675
- [20] Dür W, Vidal G and Cirac J I 2000 Three qubits can be entangled in two inequivalent ways *Phys. Rev. A* **62** 062314
- [21] Briegel H J and Raussendorf R 2001 Persistent entanglement in arrays of interacting particles *Phys. Rev. Lett.* **86** 910
- [22] Coffman V, Kundu J and Wootters W K 2000 Distributed entanglement *Phys. Rev. A* **61** 052306
- [23] Yu C-s and Song H-s 2005 Multipartite entanglement measure *Phys. Rev. A* **71** 042331
- [24] Eisert J and Briegel H J 2001 Schmidt measure as a tool for quantifying multiparticle entanglement *Phys. Rev. A* **64** 022306
- [25] Carvalho A R R, Mintert F and Buchleitner A 2004 Decoherence and multipartite entanglement *Phys. Rev. Lett.* **93** 230501
- [26] Pezzé L and Smerzi A 2009 Entanglement, nonlinear dynamics and the Heisenberg limit *Phys. Rev. Lett.* **102** 100401
- [27] Hyllus P, Laskowski W, Krischek R, Schwemmer C, Wieczorek W, Weinfurter H, Pezzé L and Smerzi A 2012 Fisher information and multiparticle entanglement *Phys. Rev. A* **85** 022321
- [28] Scali S and Franzosi R 2019 Entanglement estimation in non-optimal qubit states *Ann. Phys.* **411** 167995
- [29] Vesperini A, Bel-Hadj-Aissa G and Franzosi R 2023 Entanglement and quantum correlation measures for quantum multipartite mixed states *Sci. Rep.* **13** 2852
- [30] Vesperini A, Bel-Hadj-Aissa G, Capra L and Franzosi R 2024 Unveiling the geometric meaning of quantum entanglement: discrete and continuous variable systems *Front. Phys.* **19** 51204
- [31] Vesperini A 2023 Correlations and projective measurements in maximally entangled multipartite states *Ann. Phys., NY* **457** 169406
- [32] Nourmandipour A, Vafafard A, Mortezapour A and Franzosi R 2021 Entanglement protection of classically driven qubits in a lossy cavity *Sci. Rep.* **11** 16259
- [33] Braunstein S L and Van Loock P 2005 Quantum information with continuous variables *Rev. Mod. Phys.* **77** 513
- [34] Wang X-B, Hiroshima T, Tomita A and Hayashi M 2007 Quantum information with gaussian states, *Phys. Rep.* **448** 1–11
- [35] Weedbrook C, Pirandola S, García-Patrón R, Cerf N J, Ralph T C, Shapiro J H and Lloyd S 2012 Gaussian quantum information *Rev. Mod. Phys.* **84** 621
- [36] Adesso G, Ragy S and Lee A R 2014 Continuous variable quantum information: Gaussian states and beyond *Open Syst. Inf. Dyn.* **21** 1440001
- [37] Wald R M 1994 *Quantum Field Theory in Curved Spacetime and Black Hole Thermodynamics* (University of Chicago Press)

- [38] Parker L and Toms D 2009 *Quantum Field Theory in Curved Spacetime: Quantized Fields and Gravity* (Cambridge University Press)
- [39] Umezawa H, Matsumoto H and Tachiki M 1982 *Thermo Field Dynamics and Condensed States* (North Holland)
- [40] Blasone M, Jizba P and Vitiello G 2011 *Quantum Field Theory and its Macroscopic Manifestations: Boson Condensation, Ordered Patterns and Topological Defects* (World Scientific)
- [41] Berezin F 2012 *The Method of Second Quantization* vol 24 (Elsevier)
- [42] Guaita T, Hackl L, Shi T, Hubig C, Demler E and Cirac J I 2019 Gaussian time-dependent variational principle for the Bose-Hubbard model *Phys. Rev. B* **100** 094529
- [43] Windt B, Jahn A, Eisert J and Hackl L 2021 Local optimization on pure Gaussian state manifolds *SciPost Phys.* **10** 066
- [44] Cerezo M et al 2021 Variational quantum algorithms *Nat. Rev. Phys.* **3** 625
- [45] Chen X-y 2005 Gaussian relative entropy of entanglement *Phys. Rev. A* **71** 062320
- [46] De Palma G and Hackl L 2022 Linear growth of the entanglement entropy for quadratic Hamiltonians and arbitrary initial states *SciPost Phys.* **12** 021
- [47] Adesso G and Illuminati F 2005 Gaussian measures of entanglement versus negativities: ordering of two-mode Gaussian states *Phys. Rev. A* **72** 032334
- [48] Adesso G, Serafini A and Illuminati F 2006 Multipartite entanglement in three-mode gaussian states of continuous-variable systems: quantification, sharing structure and decoherence *Phys. Rev. A* **73** 032345
- [49] Tserkis S and Ralph T C 2017 Quantifying entanglement in two-mode Gaussian states *Phys. Rev. A* **96** 062338
- [50] Hackl L and Myers R C Circuit complexity for free fermions *J. High Energy Phys.* **JHEP07(2018)139**
- [51] Chapman S, Eisert J, Hackl L, Heller M P, Jefferson R, Marrochio H and Myers R 2019 Complexity and entanglement for thermofield double states *SciPost Phys.* **6** 034
- [52] Hackl L, Guaita T, Shi T, Haegeman J, Demler E and Cirac I 2020 Geometry of variational methods: dynamics of closed quantum systems *SciPost Phys.* **9** 048
- [53] Hackl L and Bianchi E 2021 Bosonic and fermionic Gaussian states from Kähler structures *SciPost Phys. Core* **4** 025
- [54] Nishioka T 2018 Entanglement entropy: holography and renormalization group *Rev. Mod. Phys.* **90** 035007
- [55] Calabrese P and Cardy J 2009 Entanglement entropy and conformal field theory *J. Phys. A: Math. Theor.* **42** 504005
- [56] Casini H and Huerta M 2009 Entanglement entropy in free quantum field theory *J. Phys. A: Math. Theor.* **42** 504007
- [57] Witten E 2018 Aps medal for exceptional achievement in research: invited article on entanglement properties of quantum field theory *Rev. Mod. Phys.* **90** 045003
- [58] Hollands S and Sanders K 2017 Entanglement measures and their properties in quantum field theory (arXiv:1702.04924)
- [59] Rangamani M and Takayanagi T *Holographic Entanglement Entropy* vol 931 (Springer) (arXiv:1609.01287)
- [60] Tóth G 2012 Multipartite entanglement and high-precision metrology *Phys. Rev. A* **85** 022322
- [61] Pezzè L and Smerzi A 2014 *Quantum Theory of Phase Estimation (Atom Interferometry)* (IOS Press) pp 691–741
- [62] Hauke P, Heyl M, Tagliacozzo L and Zoller P 2016 Measuring multipartite entanglement through dynamic susceptibilities *Nat. Phys.* **12** 778
- [63] Rajabpour M 2017 Multipartite entanglement and quantum Fisher information in conformal field theories *Phys. Rev. D* **96** 126007
- [64] Paris M G A, Illuminati F, Serafini A and De Siena S 2003 Purity of Gaussian states: measurement schemes and time evolution in noisy channels *Phys. Rev. A* **68** 012314
- [65] Facchi P, Florio G, Parisi G and Pascazio S 2008 Maximally multipartite entangled states *Phys. Rev. A* **77** 060304
- [66] Facchi P, Florio G, Lupo C, Mancini S and Pascazio S 2009 Gaussian maximally multipartite-entangled states *Phys. Rev. A* **80** 062311
- [67] Sen A and Sen U 2010 Channel capacities versus entanglement measures in multiparty quantum states *Phys. Rev. A* **81** 012308

- [68] Roy S, Das T and Sen A 2020 Computable genuine multimode entanglement measure: Gaussian versus non-Gaussian *Phys. Rev. A* **102** 012421
- [69] Ma Z-H, Chen Z-H, Chen J-L, Spengler C, Gabriel A and Huber M 2011 Measure of genuine multipartite entanglement with computable lower bounds *Phys. Rev. A* **83** 062325
- [70] Xie S, Younis D, Mei Y and Eberly J H 2024 Multipartite entanglement: a journey through geometry *Entropy* **26** 217
- [71] Demkowicz-Dobrzański R, Buchleitner A, Kuś M and Mintert F 2006 Evaluable multipartite entanglement measures: multipartite concurrences as entanglement monotones *Phys. Rev. A* **74** 052303
- [72] Horodecki R, Horodecki P, Horodecki M and Horodecki K 2009 Quantum entanglement *Rev. Mod. Phys.* **81** 865
- [73] Andersson E and Öhberg P 2014 *Quantum Information and Coherence* (Springer)
- [74] Scott A J 2004 Multipartite entanglement, quantum-error-correcting codes and entangling power of quantum evolutions *Phys. Rev. A* **69** 052330
- [75] Wolf M M, Giedke G, Krüger O, Werner R F and Cirac J I 2004 Gaussian entanglement of formation *Phys. Rev. A* **69** 052320
- [76] Hill S A and Wootters W K 1997 Entanglement of a pair of quantum bits *Phys. Rev. Lett.* **78** 5022
- [77] Marian P, Marian T A and Scutaru H 2003 Bures distance as a measure of entanglement for two-mode squeezed thermal states *Phys. Rev. A* **68** 062309
- [78] Marian P and Marian T A 2008 Entanglement of formation for an arbitrary two-mode Gaussian state *Phys. Rev. Lett.* **101** 220403
- [79] Tserkis S, Onoe S and Ralph T C 2019 Quantifying entanglement of formation for two-mode Gaussian states: analytical expressions for upper and lower bounds and numerical estimation of its exact value *Phys. Rev. A* **99** 052337
- [80] Plenio M B 2005 Logarithmic negativity: a full entanglement monotone that is not convex *Phys. Rev. Lett.* **95** 090503
- [81] Serafini A 2017 *Quantum Continuous Variables: a Primer of Theoretical Methods* (CRC Press)
- [82] Serafini A, Dahlsten O, Gross D and Plenio M 2007 Canonical and micro-canonical typical entanglement of continuous variable systems *J. Phys. A: Math. Theor.* **40** 9551
- [83] Fukuda M and Koenig R 2019 Typical entanglement for Gaussian states *J. Math. Phys.* **60** 112203060304
- [84] Blaizot J-P and Ripka G 1986 Quantum theory of finite systems
- [85] Bengtsson I and Życzkowski K 2017 *Geometry of Quantum States: an Introduction to Quantum Entanglement* (Cambridge University Press)
- [86] Chabaud U, Markham D and Grosshans F 2020 Stellar representation of non-Gaussian quantum states *Phys. Rev. Lett.* **124** 063605
- [87] Guaita T, Hackl L, Shi T, Demler E and Cirac J I 2021 Generalization of group-theoretic coherent states for variational calculations *Phys. Rev. Res.* **3** 023090
- [88] Rahman M and Geiger D 2016 Quantum clustering and Gaussian mixtures (arXiv:1612.09199)